

Soret Effect Through a Rotating Porous Disk of MHD Fluid Flow



Krishnandan Verma, Debozani Borgohain, B.R. Sharma

Abstract: The present study attempts to investigate numerically the problem due to rotating porous disk of MHD fluid flow with Soret effect using Darcy-Forchheimer model in a steady laminar Newtonian fluid. By using similarity transformation the governing equations of continuity, momentum, energy and concentration are converted into a system of nonlinear ODE's. Matlab's built in solver bvp4c has been employed to solve numerically the coupled ODE's. Numerical results are obtained for velocity (radial, axial and tangential), temperature and concentration profiles for various parameters and are illustrated graphically. The effect of suction parameter on the radial and tangential skin friction coefficients and rate of heat transfer are obtained and compared with the one available in literature. The results are found to be in good agreement. Numerical values of Skin-friction coefficient, Nusselt number and Sherwood number are obtained for different values of parameter.

Keywords: bvp4c, Darcy- Forchheimer, Porous rotating disk, Soret effect.

I. INTRODUCTION

The flow based on rotating disk is important from both theoretical and practical point of view. Many modern engineering types of machinery are based on rotating disk. Practical applications are seen in many areas such as laboratory where instruments are used to study reaction between fluids and solid, oceanography, viscometer, lubrication, rotating machinery and computer devices etc. The flow problem due to a rotating disk has been studied from a long time. Von Karman [1] was the pioneer to study the flow problem over an infinite rotating disk. He described similarity transformations of the flow problem in steady state which reduced the Navier Stokes equations to the system of coupled ordinary differential equations. Cochran [2] patched two series expansions and obtained more accurate results. Benton [3] extended Cochran's work and improved the solution further. After that many researchers carried out comprehensive study on flow problems due to rotating disk like Millsaps and Pohlhausen [4], Sparrow and Gregg [5], Hassan and Attia [6], Kelson and Desseaux [7], Maleque and Sattar [8] investigated unsteady, incompressible MHD convective flow over an infinite rotating disk with heat absorption effect. H.

A. Attia [9] carried numerical study due to a rotating disk on steady incompressible viscous fluid in a porous medium with heat transfer. Maleque [10] studied thermal diffusion and diffusion-thermo effect with heat and mass transfer on MHD convective fluid flow due to a rotating disk. Sharma and Borgohain [11] studied numerically heat and mass transfer under the influence of chemical reaction due to rotating disk of a binary fluid mixture in porous medium. Dhandapat and Singh [12] studied numerically unsteady flow problem in presence of uniform magnetic field over a non-uniform rotating disk on two layer film flow. EL. Dabe *et. al.* [13] investigated the problem due to infinite rotating uniform disk in nanofluid on steady MHD flow along with non linear heat and mass transfer. The rotating disk problem has been studied by many researchers in porous medium and the present study investigates the problem due to rotating porous disk using the Darcy-Forchheimer model [14]. The Forchheimer law [15] was given by an Austrian scientist Philip Forchheimer during his work on fluid flow through porous media. The objective of this paper is to study numerically Soret effect over a rotating infinite disk of MHD flow problem in porous medium considering Darcy-Forchheimer model.

II. MATHEMATICAL FORMULATION

Consider heat and mass transfer through a steady, incompressible, electrically conducting fluid flow due to a porous disk. The disk is axially symmetric and rotating with a constant angular velocity Ω . Radiation has been taken into account and the fluid is taken to be infinite in extent in the positive direction of z-axis. Let the disk be placed at $z = 0$ and cylindrical polar coordinate (r, ϕ, z) is considered. In the increasing direction of (r, ϕ, z) , the flow velocity components (u, v, w) are considered respectively. Let the temperature, concentration and pressure distribution be T , C and p respectively. Let a uniform temperature T_w and uniform concentration C_w be maintained at the surface of the disk. The free stream is maintained at a constant temperature T_∞ , constant concentration C_∞ and constant pressure p_∞ . Let the fluid be Newtonian, gray and heat absorbing.

The Maxwell's equation are:

$$\text{div } \vec{B} = 0, \text{ curl } \vec{B} = \mu_m \vec{J} \text{ and } \text{div } \vec{E} = 0$$

Revised Manuscript Received on August 30, 2020.

* Correspondence Author

Krishnandan Verma*, Department of Mathematics, Dibrugarh University, Assam, India.

Debozani Borgohain, Assistant Professor, Department of Mathematics, Dibrugarh University, Dibrugarh, Assam, India.

Dr. B. R. Sharma, Department of Mathematics, Dibrugarh University, Assam, India.

© The Authors. Published by Blue Eyes Intelligence Engineering and Sciences Publication (BEIESP). This is an open access article under the CC BY-NC-ND license (<http://creativecommons.org/licenses/by-nc-nd/4.0/>)



where $\bar{B} = B + b$ is the total magnetic field, \bar{J} is current density, μ_m is magnetic permeability, B is external uniform magnetic field and b is the induced magnetic field.

In the normal direction to the surface of the disk an external uniform magnetic field is applied which remains unchanged by a small magnitude of magnetic Reynolds number. Also at the surface of the disk a uniform suction is applied

. The MHD body force $\bar{J} \times \bar{B}$ is given by,

$$\sigma(\bar{V} \times \bar{B}) \times \bar{B} = -\sigma B^2 \bar{V} / r, \quad \text{where } \bar{V} = (u, v, w), \\ \bar{B} = (0, 0, B) \text{ and } \sigma \text{ is the electrical conductivity of the fluid. There are two components of Lorentz force,} \\ F_r = -\sigma B^2 u / r \text{ and } F_\theta = -\sigma B^2 v / r.$$

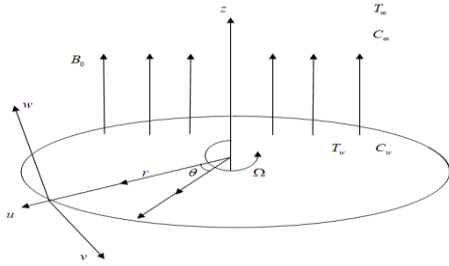


Fig 1. Geometry of the problem

The governing equations are

$$\frac{\partial u}{\partial r} + \frac{u}{r} + \frac{\partial w}{\partial z} = 0, \quad (1)$$

$$u \frac{\partial u}{\partial r} - \frac{v^2}{r} + w \frac{\partial u}{\partial z} = -\frac{1}{\rho} \frac{\partial p}{\partial r} + \\ v \left(\frac{\partial^2 u}{\partial r^2} + \frac{1}{r} \frac{\partial u}{\partial r} - \frac{u}{r^2} + \frac{\partial^2 u}{\partial z^2} \right) - \frac{\sigma B^2}{\rho r} u \\ - \frac{\nu}{K_1^*} u + g \beta_T (T - T_\infty) + g \beta_C (C - C_\infty) \\ - \frac{C_F}{(K_1^*)^2} \rho \sqrt{u^2 + v^2 + w^2} u, \quad (2)$$

$$u \frac{\partial v}{\partial r} + \frac{uv}{r} + w \frac{\partial v}{\partial z} = v \left(\frac{\partial^2 v}{\partial r^2} + \frac{1}{r} \frac{\partial v}{\partial r} - \frac{v}{r^2} + \frac{\partial^2 v}{\partial z^2} \right) \\ - \frac{\sigma B^2}{\rho r} v - \frac{\nu}{K_1^*} v - \frac{C_F}{(K_1^*)^2} \rho \sqrt{u^2 + v^2 + w^2} v, \quad (3)$$

$$u \frac{\partial w}{\partial r} + w \frac{\partial w}{\partial z} = -\frac{1}{\rho} \frac{\partial p}{\partial z} + v \left(\frac{\partial^2 w}{\partial r^2} + \frac{1}{r} \frac{\partial w}{\partial r} + \frac{\partial^2 w}{\partial z^2} \right) \\ - \frac{\nu}{K_1^*} w - \frac{C_F}{(K_1^*)^2} \rho \sqrt{u^2 + v^2 + w^2} w, \quad (4)$$

$$u \frac{\partial T}{\partial r} + w \frac{\partial T}{\partial z} = \frac{k}{\rho c_p} \left(\frac{\partial^2 T}{\partial r^2} + \frac{1}{r} \frac{\partial T}{\partial r} + \frac{\partial^2 T}{\partial z^2} \right) - \frac{1}{\rho c_p} \frac{\partial q_r}{\partial z}$$

$$+ \frac{Dk_T}{c_s c_p} \left(\frac{\partial^2 C}{\partial r^2} + \frac{1}{r} \frac{\partial C}{\partial r} + \frac{\partial^2 C}{\partial z^2} \right) + \frac{\sigma B^2}{\rho c_p r^3} u^2 \\ + \frac{Q}{\rho c_p} (T - T_\infty), \quad (5)$$

$$u \frac{\partial C}{\partial r} + w \frac{\partial C}{\partial z} = D \left(\frac{\partial^2 C}{\partial r^2} + \frac{1}{r} \frac{\partial C}{\partial r} + \frac{\partial^2 C}{\partial z^2} \right) \\ + \frac{Dk_T}{T_m} \left(\frac{\partial^2 T}{\partial r^2} + \frac{1}{r} \frac{\partial T}{\partial r} + \frac{\partial^2 T}{\partial z^2} \right) - k_1 (C - C_\infty). \quad (6)$$

where $\rho, \nu, K_1^*, \beta_T, \beta_C, C_F, g, q_r, D, k_T, c_p, c_s, Q, T_m$ and k_1 represents the fluid density, kinematic viscosity, permeability of the porous medium, coefficient of temperature, coefficient of concentration, drag constant, acceleration due to gravity, radiative heat flux, molecular diffusion coefficient, thermal diffusion rate, specific heat at constant pressure, concentration susceptibility, rate of volumetric heat generation/absorption, mean fluid temperature and rate of chemical reaction respectively.

The expression for tangential velocity, U_t (Gad-el-Hak [16]) is given by:

$$U_t = \frac{2 - \xi}{\xi} \lambda \frac{\partial U_t}{\partial n}. \quad (7)$$

Boundary conditions are obtained by using equation (7) as:

$$z = 0: u = \frac{2 - \xi}{\xi} \lambda \frac{\partial u}{\partial z}, v = \Omega r + \frac{2 - \xi}{\xi} \lambda \frac{\partial v}{\partial z}, \\ w = w_0, \quad T = T_w, \quad C = C_w, \\ z \rightarrow \infty: u \rightarrow 0, \quad v \rightarrow 0, \quad T \rightarrow T_\infty, \quad C \rightarrow C_\infty, \\ p \rightarrow p_\infty. \quad (8)$$

where ξ, λ and Ω represents tangent momentum accommodation coefficient, mean free path and constant angular velocity respectively.

Using Rosseland mean absorption coefficient, the Radiative heat flux, q_r is given by

$$q_r = -\frac{4\sigma^*}{3k^*} \frac{\partial T^4}{\partial z}. \quad (9)$$

where σ^* and k^* are Stephan-Boltzmann constant and Rosseland mean absorption coefficient respectively.

Within the flow there is minor temperature difference, so T^4 can be expressed as

$$T^4 \cong 4T_\infty^3 T - 3T_\infty^4. \quad (10)$$

Magnetic field $B(r)$ in our above study (Cobble [17]) is

given by, $B = B_0 \sqrt{r}$ where B_0 is the constant magnetic flux density.

The following similarity transformations are used to make the above equations non dimensional.

$$\begin{aligned} \bar{R} &= \frac{r}{L}, \quad \bar{Z} = \frac{z}{L}, \quad \bar{U} = \frac{u}{\Omega L}, \quad \bar{V} = \frac{v}{\Omega L}, \quad \bar{\lambda} = \frac{\lambda}{L}, \\ \bar{W} &= \frac{w}{\Omega L}, \quad \bar{P} = \frac{p - p_\infty}{\rho \Omega^2 L^2}, \quad \bar{\nu} = \frac{\nu}{\Omega L^2}, \quad k_1 = \frac{\bar{k}_1}{L^2}, \\ \bar{T} &= \frac{T - T_\infty}{T_w - T_\infty}, \quad \bar{C} = \frac{C - C_\infty}{C_w - C_\infty}, \quad \bar{K}_1^* = \frac{K_1^*}{L^2}. \end{aligned} \quad (11)$$

Using the equations (9)-(11) in equations (1)-(6), the dimensionless equations obtained are:

$$\frac{\partial \bar{U}}{\partial \bar{R}} + \frac{\bar{U}}{\bar{R}} + \frac{\partial \bar{W}}{\partial \bar{Z}} = 0, \quad (12)$$

$$\begin{aligned} \bar{U} \frac{\partial \bar{U}}{\partial \bar{R}} - \frac{\bar{V}^2}{\bar{R}} + \bar{W} \frac{\partial \bar{U}}{\partial \bar{Z}} &= -\frac{\partial \bar{P}}{\partial \bar{R}} + \\ &\bar{\nu} \left(\frac{\partial^2 \bar{U}}{\partial \bar{R}^2} + \frac{1}{\bar{R}} \frac{\partial \bar{U}}{\partial \bar{R}} - \frac{\bar{U}}{\bar{R}^2} + \frac{\partial^2 \bar{U}}{\partial \bar{Z}^2} \right) - \frac{\sigma B_0^2}{\rho \Omega} \bar{U} \\ &- \frac{\bar{\nu}}{\bar{K}_1^*} \bar{U} + \frac{g \beta_T (T_w - T_\infty)}{\Omega^2 L} \bar{T} + \frac{g \beta_C (C_w - C_\infty)}{\Omega^2 L} \bar{C} \\ &- \frac{C_F}{(\bar{K}_1^*)^2} \rho \sqrt{\bar{U}^2 + \bar{V}^2 + \bar{W}^2} \bar{U}, \end{aligned} \quad (13)$$

$$\begin{aligned} \bar{U} \frac{\partial \bar{V}}{\partial \bar{R}} + \frac{\bar{U} \bar{V}}{\bar{R}} + \bar{W} \frac{\partial \bar{V}}{\partial \bar{Z}} &= \bar{\nu} \left(\frac{\partial^2 \bar{V}}{\partial \bar{R}^2} + \frac{1}{\bar{R}} \frac{\partial \bar{V}}{\partial \bar{R}} - \frac{\bar{V}}{\bar{R}^2} + \frac{\partial^2 \bar{V}}{\partial \bar{Z}^2} \right) \\ &- \frac{\sigma B_0^2}{\rho \Omega} \bar{V} - \frac{\bar{\nu}}{\bar{K}_1^*} \bar{V} - \frac{C_F}{(\bar{K}_1^*)^2} \rho \sqrt{\bar{U}^2 + \bar{V}^2 + \bar{W}^2} \bar{V}, \end{aligned} \quad (14)$$

$$\begin{aligned} \bar{U} \frac{\partial \bar{W}}{\partial \bar{R}} + \bar{W} \frac{\partial \bar{W}}{\partial \bar{Z}} &= -\frac{\partial \bar{P}}{\partial \bar{Z}} + \bar{\nu} \left(\frac{\partial^2 \bar{W}}{\partial \bar{R}^2} + \frac{1}{\bar{R}} \frac{\partial \bar{W}}{\partial \bar{R}} + \frac{\partial^2 \bar{W}}{\partial \bar{Z}^2} \right) \\ &- \frac{\bar{\nu}}{\bar{K}_1^*} \bar{W} - \frac{C_F}{(\bar{K}_1^*)^2} \rho \sqrt{\bar{U}^2 + \bar{V}^2 + \bar{W}^2} \bar{W}, \end{aligned} \quad (15)$$

$$\begin{aligned} \bar{U} \frac{\partial \bar{T}}{\partial \bar{R}} + \bar{W} \frac{\partial \bar{T}}{\partial \bar{Z}} &= \frac{k}{\rho c_p L^2 \Omega} \left(\frac{\partial^2 \bar{T}}{\partial \bar{R}^2} + \frac{1}{\bar{R}} \frac{\partial \bar{T}}{\partial \bar{R}} + \frac{\partial^2 \bar{T}}{\partial \bar{Z}^2} \right) \\ &+ \frac{16 \sigma^* T_\infty^3}{3 \rho c_p k^* \Omega L^2} \frac{\partial^2 \bar{T}}{\partial \bar{Z}^2} \\ &+ \frac{Dk_T}{c_s c_p \Omega L^2} \frac{(C_w - C_\infty)}{(T_w - T_\infty)} \left(\frac{\partial^2 \bar{C}}{\partial \bar{R}^2} + \frac{1}{\bar{R}} \frac{\partial \bar{C}}{\partial \bar{R}} + \frac{\partial^2 \bar{C}}{\partial \bar{Z}^2} \right) \\ &+ \frac{\sigma B_0^2 \Omega L}{\rho c_p (T_w - T_\infty)} \frac{\bar{U}^2}{\bar{R}^2} + \frac{Q}{\rho c_p \Omega} \bar{T}, \end{aligned} \quad (16)$$

$$\begin{aligned} \bar{U} \frac{\partial \bar{C}}{\partial \bar{R}} + \bar{W} \frac{\partial \bar{C}}{\partial \bar{Z}} &= \frac{D}{\Omega L^2} \left(\frac{\partial^2 \bar{C}}{\partial \bar{R}^2} + \frac{1}{\bar{R}} \frac{\partial \bar{C}}{\partial \bar{R}} + \frac{\partial^2 \bar{C}}{\partial \bar{Z}^2} \right) \\ &+ \frac{Dk_T (T_w - T_\infty)}{T_m \Omega L^2 (C_w - C_\infty)} \left(\frac{\partial^2 \bar{T}}{\partial \bar{R}^2} + \frac{1}{\bar{R}} \frac{\partial \bar{T}}{\partial \bar{R}} + \frac{\partial^2 \bar{T}}{\partial \bar{Z}^2} \right) - \frac{\bar{k}_1}{\Omega L^2} \bar{C}. \end{aligned} \quad (17)$$

The boundary conditions are

$$\begin{aligned} \bar{Z} = 0: \quad \bar{U} &= \frac{2-\xi}{\xi} \bar{\lambda} \frac{\partial \bar{U}}{\partial \bar{Z}}, \quad \bar{V} = \bar{R} + \frac{2-\xi}{\xi} \bar{\lambda} \frac{\partial \bar{V}}{\partial \bar{Z}}, \\ \bar{W} &= \frac{w_0}{\Omega L}, \quad \bar{T} = 1, \quad \bar{C} = 1, \\ \bar{Z} \rightarrow \infty: \quad \bar{U} &\rightarrow 0, \quad \bar{V} \rightarrow 0, \quad \bar{T} \rightarrow 0, \quad \bar{C} \rightarrow 0, \quad \bar{P} \rightarrow 0. \end{aligned} \quad (18)$$

Von-Karman transformations are used along with $\eta = \frac{\bar{Z}}{\sqrt{\bar{V}}}$, a non-dimensional normal distance from the disk to obtain the governing equations,

$$\begin{aligned} \bar{U} &= \bar{R} F(\eta), \quad \bar{V} = \bar{R} G(\eta), \quad \bar{W} = \sqrt{\bar{V}} H(\eta), \\ \bar{T} &= \theta(\eta), \quad \bar{C} = \varphi(\eta), \quad \bar{P} = \bar{\nu} \bar{P}(\eta) \end{aligned} \quad (19)$$

where F, G, H, θ, φ and \bar{P} are expressed as dimensionless function of vertical coordinate η . The non-linear ODE obtained by using the transformations is as follows:

$$2F + H' = 0, \quad (20)$$

$$F'' - HF' - F^2 + G^2 - (M + S)F + \alpha\theta + N\varphi - A_1 \sqrt{F^2 + G^2 + \frac{H^2}{R_e}} F = 0, \quad (21)$$

$$G'' - HG' - 2FG - (M + S)G - A_1 \sqrt{F^2 + G^2 + \frac{H^2}{R_e}} G = 0, \quad (22)$$

$$H'' - HH' - \bar{P}' - SH - A_1 \sqrt{F^2 + G^2 + \frac{H^2}{R_e}} H = 0, \quad (23)$$

$$\frac{1}{P_r} \left(1 + \frac{4}{3R} \right) \theta'' - H\theta' + D_f \varphi'' + JF^2 + \delta\theta = 0, \quad (24)$$

$$\frac{1}{S_c} \varphi'' - H\varphi' + S_r \theta'' - \beta\varphi = 0. \quad (25)$$

Where $A_1 = \frac{C_F}{(\bar{K}^*)^2} \rho \bar{R}, M = \sigma B_0^2 / \rho \Omega,$

$$N = g\beta_c (C_w - C_\infty) / \bar{L} \bar{R} \Omega^2, S = \bar{v} / \bar{k}_1^*, S_c = \nu / D,$$

$$D_f = Dk_T (C_w - C_\infty) / \nu c_p (T_w - T_\infty), S_r = Dk_T (T_w - T_\infty) / \nu T_m (C_w - C_\infty),$$

$$R = R_d^{-1} = k^* k / 4\sigma^* T_\infty^3, R_e = \bar{R}^2 / \bar{v}, P_r = \nu \rho c_p / k,$$

$$\alpha = g\beta_T (T_w - T_\infty) / \bar{L} \bar{R} \Omega^2, \delta = Q / \Omega \rho c_p, \beta = \bar{k} / \Omega L^2$$

and $J = \sigma B_0^2 \Omega L / \rho c_p (T_w - T_\infty)$ represents Darcy-

Forchheimer parameter, Magnetic parameter, concentration buoyancy parameter, porosity parameter, Schmidt number,

Dufour number, Soret number, Radiation parameter, Rotational Reynold's number, Prandtl number, Temperature buoyancy parameter, Heat source parameter, chemical reaction parameter and Joule heating parameter. The modified boundary conditions are:

$$\eta = 0; F(0) = \gamma F'(0), G(0) = 1 + \gamma G'(0),$$

$$H(0) = W_s, \theta(0) = 1, \varphi(0) = 1,$$

$$\eta \rightarrow \infty; F(\infty) = 0, G(\infty) = 0, \theta(\infty) = 0,$$

$$\varphi(\infty) = 0, \bar{P}(\infty) = 0. \quad (26)$$

where slip factor, $\gamma = \left[(2 - \xi) \lambda \sqrt{\Omega} \right] / \xi \sqrt{\nu}$ and uniform suction at the disk $W_s = w_0 / \sqrt{\nu \Omega}, (W_s < 0)$.

The skin-friction coefficient, Nusselt number and Sherwood number are given by:

$$\text{Tangential shear stress, } \tau_{\varphi z} = \mu \left(\frac{\partial v}{\partial z} + \frac{1}{r} \frac{\partial w}{\partial \varphi} \right)_{z=0}, \quad (27)$$

$$\text{Radial shear stress, } \tau_{rz} = \mu \left(\frac{\partial u}{\partial z} + \frac{\partial w}{\partial r} \right)_{z=0}, \quad (28)$$

Tangential skin friction coefficient,

$$C_{f_1} = \tau_{\varphi z} / \rho \Omega^2 L^2 = \bar{R}^2 \bar{v} G'(0) \approx G'(0), \quad (29)$$

Radial skin friction coefficient,

$$C_{f_2} = \tau_{rz} / \rho \Omega^2 L^2 = \bar{R}^2 \bar{v} F'(0) \approx F'(0), \quad (30)$$

$$\text{Heat flux at the surface, } q_w = -k \left(\frac{\partial T}{\partial z} \right)_{z=0}, \quad (31)$$

$$\text{Mass flux at the surface, } M_w = -D \left(\frac{\partial C}{\partial z} \right)_{z=0}, \quad (32)$$

$$\text{Nusselt number, } N_u = \frac{L q_w}{k (T_w - T_\infty) (\bar{v})^{-1/2}} = -\theta'(0), \quad (33)$$

$$\text{Sherwood number, } S_h = \frac{LM_w}{D(C_w - C_\infty)(\bar{v})^{-1/2}} = -\phi'(0). \quad (34)$$

III. NUMERICAL SOLUTION AND DISCUSSIONS

Matlab's bvp4c solver has been employed to solve numerically the system of non-linear ODE's (20)-(25) along with the boundary conditions (26). The graph of the velocity (radial, axial and tangential), temperature and concentration profiles are obtained for various values of the parameter S_r , A_1 and W_s . To verify the accuracy of the numerical solution, the present results are compared with Maleque and Sattar (2005), Osalusi and Sibanda (2006) and Frusteri and Osalusi (2007) and have been shown in Table 1,2,3. The results obtained in the present study are found to be in good agreement. Numerical calculations of skin friction coefficient and heat and mass transfer rate are also carried out and are shown in table 4.

Table 1,2,3 represents comparisons of present and recent numerical value of the radial and tangential skin friction coefficients and the rate of heat transfer coefficients for various values of W_s with $S = 0$, $\alpha = 0$, $N = 0$, $J = 0$, $\delta = 0$, $P_r = 0.71$, $\beta = 0$, $R_d = 10^9$, $D_f = 0$, $S_r = 0$, $S_c = 1$, $A_1 = 0$, $R_e = 1$ and $M = 1$.

Table 1.

W_s	Frusteri <i>et. al.</i>	Osalusi <i>et. al.</i>	Maleque <i>et. al.</i>	Present study
	$F'(0)$	$F'(0)$	$F'(0)$	$F'(0)$
0.0	0.4241	0.4241	0.5102	0.5080
-2.0	0.2324	0.2324	0.2425	0.2424
-4.0	0.1246	0.1246	0.1248	0.1247
-5.0	0.0999	0.0999	0.0999	0.0999
-10.0	0.0499	0.0499	0.0506	0.0500

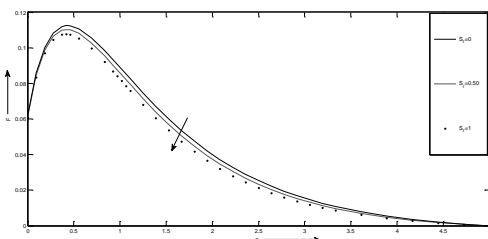


Fig 2. Radial velocity profiles versus η

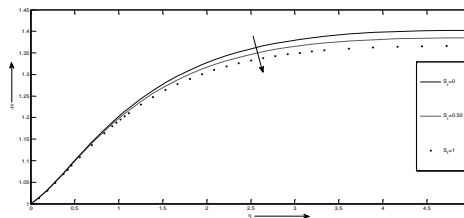


Fig 3. Axial velocity profiles versus η

Table 2.

W_s	Frusteri <i>et. al.</i>	Osalusi <i>et. al.</i>	Maleque <i>et. al.</i>	Present study
	$-G'(0)$	$-G'(0)$	$-G'(0)$	$-G'(0)$
0.0	0.6514	0.6514	0.6160	0.6149
-2.0	2.0687	2.0687	2.0391	2.0386
-4.0	4.0065	4.0065	4.0054	4.0052
-5.0	5.0029	5.0029	5.0031	5.0027
-10.0	10.0003	10.0003	10.0017	10.0003

Table 3.

W_s	Frusteri <i>et. al.</i>	Osalusi <i>et. al.</i>	Maleque <i>et. al.</i>	Present study
	$-\theta'(0)$	$-\theta'(0)$	$-\theta'(0)$	$-\theta'(0)$
0.0	0.5387	0.5387	0.3258	0.3473
-2.0	1.5196	1.5196	1.4421	1.4388
-4.0	2.8520	2.8520	2.8447	2.8424
-5.0	3.5541	3.5541	3.5541	3.5512
-10.0	7.1002	7.1002	7.1020	7.1002

Numerical Values of Skin-friction coefficient, $(-C_{f_1}, C_{f_2})$

, Nusselt number, N_u and Sherwood number, S_h at the surface for $M = 0.1, S = 2.0, \alpha = 0.5, N = 0.5, P_r = 1, D_f = 0.25, R_d = 5, J = 0.5, \delta = 0, \beta = 0.5, S_c = 0.64, \gamma = 0.2$ and $R_e = 1$.

Table 4:

S_r	W_s	A_1	$-C_{f_1}$	C_{f_2}	$-N_u$	$-S_h$
0.2	-1	0.25	1.5509	0.4025	0.7708	0.7991
0.2	-1	0.50	1.5857	0.3830	0.7636	0.7970
0.2	-1	1	1.6495	0.3503	0.7515	0.7937
0.02	-1	1	1.6497	0.3520	0.7372	0.7821
0.25	-1	1	1.6494	0.3498	0.7556	0.7970
1	-1	1	1.6480	0.3421	0.8243	0.8511
0.2	-1	1	1.6495	0.3503	0.7515	0.7937
0.2	-1.5	1	1.8293	0.3070	1.0459	0.8847
0.2	-2.0	1	1.9982	0.2676	1.3624	0.9859

Figures 2 - 6 illustrate the effect of Soret number on velocity (radial and axial), temperature and concentration profiles for $S_r = [0, 0.50, 1]$, $M = 1$, $\alpha = 0.5$, $N = 0.5$, $S = 2$, $P_r = 1$, $R_d = 5$, $D_f = 0.25$, $J = 0.5$, $\delta = 0$, $S_c = 0.64$, $\beta = 0.5$, $A_1 = 1$, $R_e = 1$, $W_s = -1$ and $\gamma = 0.2$.

From the figures it is observed that near the surface the radial velocity increases to its maximum at about $\eta = 0.5$ but decreases asymptotically thereafter at the end of the boundary layer. The temperature and the concentration decreases exponentially from the peak value at the surface to the minimum value with the increase in the value of η at the end of the boundary layer. The axial velocity also decreases with the increase in Soret number. The increasing values of Soret number do not affect the tangential velocity component.

Figures 7 - 11 represent the effect of Darcy-Forchheimer parameter on velocity (radial, axial and tangential), temperature and concentration profiles for $A_1 = [0, 0.50, 1]$, $M = 1$, $\alpha = 0.5$, $N = 0.5$, $S = 2$, $P_r = 1$, $D_f = 0.25$, $S_r = 0.2$, $S_c = 0.64$, $J = 0.5$, $\delta = 0$, $R_d = 5$, $R_e = 1$, $\beta = 0.5$, $W_s = -1$ and $\gamma = 0.2$.

It is observed from the figures that the velocity component along radial, axial and tangential directions decrease with the increase in the values of Darcy-Forchheimer parameter whereas the temperature and concentration profile increases.

Figures 12 - 16 illustrate the effect of suction parameter on velocity (radial, axial and tangential), temperature and concentration profiles

for $W_s = [-1, -1.5, -2]$, $M = 1$, $N = 0.5$, $\alpha = 0.5$, $S = 2$, $P_r = 1$, $D_f = 0.25$, $S_r = 0.2$, $S_c = 0.64$, $J = 0.5$, $\delta = 0$, $R_d = 5$, $A_1 = 1$, $R_e = 1$, $\beta = 0.5$, and $\gamma = 0.2$.

It is observed that the velocity components along radial and tangential direction, temperature and concentration profiles decrease with the increase in suction parameter whereas the axial component of velocity increases. The increase in suction parameter reduces concentration and thermal boundary layer due to which reduction in temperature and concentration is noticed.

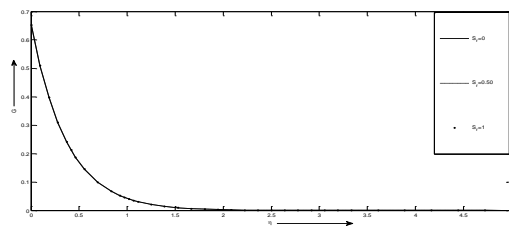


Fig 4. Tangential velocity profiles versus η

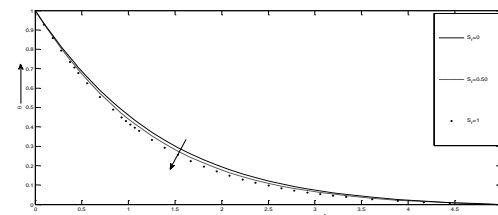


Fig 5. Temperature profiles versus η

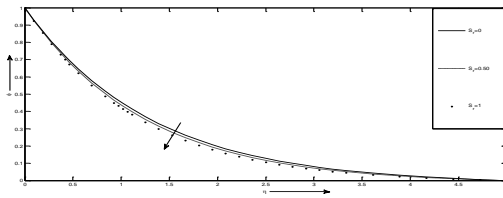


Fig 6. Concentration velocity profiles versus η

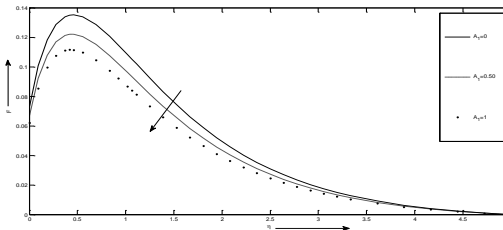


Fig 7. Radial velocity profiles versus η

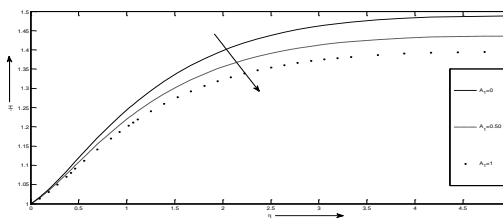


Fig 8. Axial velocity profiles versus η

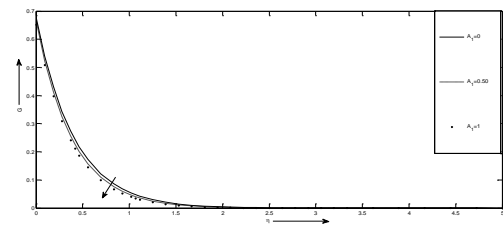


Fig 9. Tangential velocity profiles versus η

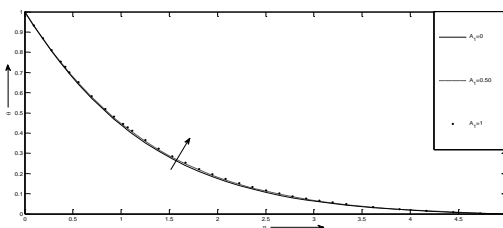


Fig 10. Temperature profiles versus η

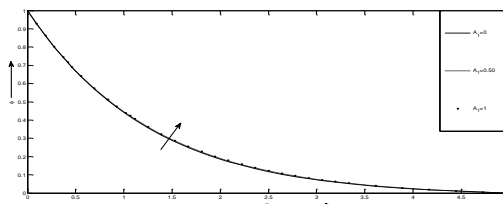


Fig 11. Concentration profiles versus η

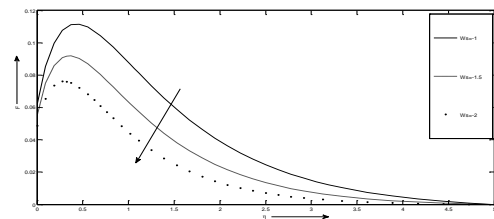


Fig 12. Radial velocity profiles versus η

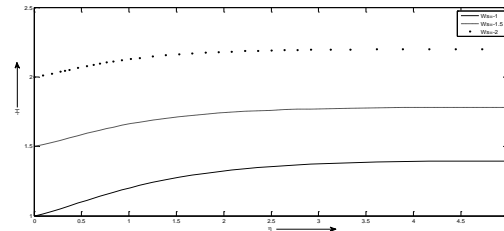


Fig 13. Axial velocity profiles versus η

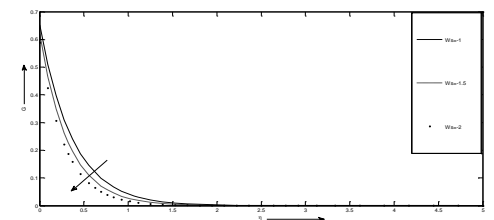


Fig 14. Tangential velocity profiles versus η

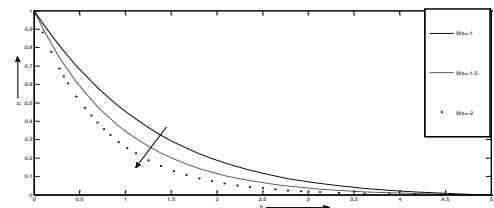


Fig 15. Temperature profiles versus η

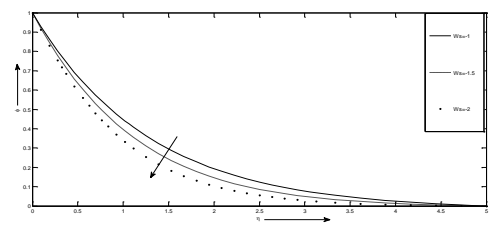


Fig 16. Concentration profiles versus η

IV. CONCLUSION

From the above discussions the following outcomes are derived:

1. The radial component of velocity decreases with the increasing values of the parameters S_r , A_1 and W_s .
2. The axial velocity component increases for the increasing values of W_s but decreases with the increasing values of S_r and A_1 .

3. The tangential component of velocity decreases for the increasing values of A_1 and W_s .
4. The temperature of the fluid increases with the increasing values A_1 but decreases with the increasing values of S_r and W_s .
5. The concentration of the fluid increases with the increase in the values of A_1 but decreases with the increasing values of the parameters S_r and W_s .
6. The increase in the value of Darcy-Forchheimer parameter, A_1 increases the tangential skin-friction $(-G'(0))$ but decreases the radial skin-friction $(F'(0))$, heat transfer rate $(-\theta'(0))$ and mass transfer rate $(-\phi'(0))$.
7. The increase in the value of Soret number, S_r decreases the tangential skin friction $(-G'(0))$ and radial skin friction $(F'(0))$ but increases heat transfer rate $(-\theta'(0))$ and mass transfer rate $(-\phi'(0))$.
8. The decrease in the value of Suction parameter, W_s increases the tangential skin-friction $(-G'(0))$, heat transfer rate $(-\theta'(0))$ and mass transfer rate $(-\phi'(0))$ but decreases the radial skin friction $(F'(0))$.

REFERENCES

1. Von Karman T. Uber, 1921, "Laminare und turbulente Reibung. Zeitschrift für Angewandte Mathematik und Mechanik", 1:1233-1255.
2. Cochran WG., 1934, "The flow due to a rotating disk". Proceedings of the Cambridge Philosophical Society, 30:365-375.
3. Benton ER., 1966, "On the flow due to a rotating disk", Journal of Fluid Mechanics, 24:781-800.
4. Millsaps, K and Pohlhausen, K., 1952, "Heat transfer by laminar flow from a rotating disk", J. Aeronaut. Sci., 19, pp.120-126.
5. Sparrow, E. M., and Gregg, J.L., 1960, "Mass transfer, flow and heat transfer about a rotating disk", ASME J. Heat transfer, Nov., 294-302.
6. Hassan, A.L.A. and H.A. Attia, 1997, "Flow due to a rotating disk with Hall effect," *Physics Letters A*, 228, 246-290.
7. Kelson, N. and A. Desseaux, 2000, "Notes on porous rotating disk flow," ANZIAM J., 42(E), C837-C855.
8. Maleque, Kh.A. and M.A. Sattar, 2003, "Transient Convective Flow Due to a Rotating Disc with Magnetic Field and Heat Absorption Effects," *Journal of Energy, Heat and Mass Transfer*, 25, 279-291.
9. Attia, H.A., 2009, "Steady flow over a rotating disk in porous medium with heat transfer nonlinear analysis", *Modelling and Control*, Vol. 14, No. 1, 21-26.
10. Maleque, Kh. A., 2010, "Dufour and Soret effects on unsteady MHD convective heat and mass transfer flow due to rotating disk", *Latin American Applied Research*, 40:105-111.
11. Sharma, B.R. and Borgohain, D., 2014, "Influence of Chemical reaction, Soret and Dufour effects on heat and mass transfer of a binary fluid mixture in porous medium over a rotating disk", *IOSR Journal of Mathematics*, e-ISSN: 2278-5728, p-ISSN: 2319-765X. Vol. 10(6) Ver III, 73-78.
12. Dhanpat, B. S. and Singh, S.K., 2015, "Unsteady two layer film flow on a non uniform rotating disk in presence uniform transverse magnetic field", *Applied Mathematics and Computation*, Vol. 258, 545-555.
13. EL-Dabe, Nabil, T., Hazim A. Attia and Mohamed A. I. Essawy, Ibrahim H. Abd-elmaksoud, Ahmed A. Ramadan and Alaa H.

- Abdel-Hamid, 2019, "Non-linear heat and mass transfer in a thermal radiated MHD flow of a power-law nanofluid over a rotating disk", *SN Applied Sciences* (online), 1:551.
14. Nield, D. A. and Bejan, A., 2006, "Convection in Porous Media", Third edition, ISBN: 0-387-29096-6, 978-0387-29096-6, 1-14.
15. P. Forchheimer., 1901, *Wasserbewegung durch Boden*. Zeitschrift des Vereines Deutscher Ingenieur, 45 edition.
16. Gad-el-Hak M., 1999, "The fluid mechanics of microdevices". The freeman scholar lecture. *Journal of Fluids Engineering-Transactions of the ASME* ;121: 5-33.
17. Cobble MH., 1977, "Magnetohydrodynamic flow with a pressure gradient and fluid injection", *Journal of Engineering Mathematics*, 11:249-256.
18. Maleque A. K., Sattar A. M., 2005, "Steady laminar convective flow with variable properties due to a porous rotating disk", *Journal of Heat Transfer*; 127: 1406-1409.
19. Osalusi E, Sibanda P., 2006, "On variable laminar convective flow properties due to a porous rotating disk in a magnetic field", *Romanian Journal of Physics*, 51 (9-10): 933-944.
20. Frusteri F, Osalusi E., 2007, "On MHD and slip flow over a rotating porous disk with variable properties", *International Communications in Heat and Mass Transfer*, 14:34, 492-501.

AUTHORS PROFILE



Krishnandan Verma is currently a Research Scholar in Department of Mathematics, Dibrugarh University, Assam, India. He pursued his Bachelor's (Honours) from Nanda Nath Saikia college, Jorhat and Msc and M.Phil from Dibrugarh University. His area of interest is fluid dynamics, MHD and Heat and Mass transfer.



Debozani Borgohain is currently working as an Assistant Professor in Department of Mathematics, Dibrugarh University, Dibrugarh, Assam, India. Formerly she was working as an Assistant Professor in Jorhat Institute of Science and Technology, Jorhat, Assam for three years. She has obtained her Ph.D. from Dibrugarh University, pursued Bachelor's (Honours) degree from Indraprastha College for Women, University of Delhi and Master's degree from Gauhati University in Mathematics. Till now, she has 9 publications



Dr. B. R. Sharma is currently professor in Department of Mathematics, Dibrugarh University and also Dean of Faculty of Science and Engineering. His areas of interest are Fluid Dynamics, Heat and Mass transfer, Porous media flow and MHD. He acted formerly as head, Dept. of Mathematics, Dibrugarh University, Chief editor of Mathematical Forum, Co-ordinator of UGC SAP DRS (I), Principal investigator of UGC Major Research Project entitled "Effects of pressure gradient and temperature gradient on separation of binary fluid mixture". He has authored the book *Tensor Analysis-a primer*. He has published more than sixty research papers in national and international journals and guided ten research scholars leading to their Ph.D Degrees.